

# GPS-Synchronized Monitoring of Supernova Bursts in PandaX-4T: Enabling a Neutrino Trigger for Multi-Messenger Astronomy

Binyu Pang,<sup>2,3</sup> Zihao Bo,<sup>4</sup> Wei Chen,<sup>4</sup> Xun Chen,<sup>1,5,6</sup> Yunhua Chen,<sup>7,6</sup> Chen Cheng,<sup>8</sup> Xiangyi Cui,<sup>1</sup> Manna Deng,<sup>9</sup> Yingjie Fan,<sup>10</sup> Deqing Fang,<sup>11</sup> Xuanye Fu,<sup>4</sup> Zhixing Gao,<sup>4</sup> Yujie Ge,<sup>9</sup> Lisheng Geng,<sup>8,12,13,14</sup> Karl Giboni,<sup>4,6</sup> Xunan Guo,<sup>8</sup> Xuyuan Guo,<sup>7,6</sup> Zichao Guo,<sup>8</sup> Chencheng Han,<sup>1</sup> Ke Han,<sup>4,5,6</sup> Changda He,<sup>4</sup> Jinrong He,<sup>7</sup> Houqi Huang,<sup>15</sup> Junting Huang,<sup>4,6</sup> Yule Huang,<sup>4</sup> Ruquan Hou,<sup>5,6</sup> Xiangdong Ji,<sup>16</sup> Yonglin Ju,<sup>17,6</sup> Xiaorun Lan,<sup>18</sup> Chenxiang Li,<sup>4</sup> Jiafu Li,<sup>19</sup> Mingchuan Li,<sup>7,6</sup> Peiyuan Li,<sup>4</sup> Shuaijie Li,<sup>7,4,6</sup> Tao Li,<sup>15</sup> Yangdong Li,<sup>4</sup> Zhiyuan Li,<sup>9</sup> Qing Lin,<sup>20,18</sup> Jianglai Liu,<sup>1,21,5,6,\*</sup> Yuanchun Liu,<sup>4</sup> Congcong Lu,<sup>17</sup> Xiaoying Lu,<sup>2,3</sup> Lingyin Luo,<sup>22</sup> Yunyang Luo,<sup>18</sup> Yugang Ma,<sup>11</sup> Yajun Mao,<sup>22</sup> Yue Meng,<sup>4,5,6</sup> Ningchun Qi,<sup>7,6</sup> Zhicheng Qian,<sup>4</sup> Xiangxiang Ren,<sup>2,3</sup> Dong Shan,<sup>23</sup> Xiaofeng Shang,<sup>4</sup> Xiyuan Shao,<sup>23</sup> Guofang Shen,<sup>8</sup> Manbin Shen,<sup>7,6</sup> Wenliang Sun,<sup>7,6</sup> Xuyan Sun,<sup>4</sup> Yi Tao,<sup>24</sup> Yueqiang Tian,<sup>8</sup> Yuxin Tian,<sup>4</sup> Anqing Wang,<sup>2,3</sup> Guanbo Wang,<sup>4</sup> Hao Wang,<sup>4</sup> Haoyu Wang,<sup>4</sup> Jiamin Wang,<sup>1</sup> Lei Wang,<sup>25</sup> Meng Wang,<sup>2,3</sup> Qihong Wang,<sup>11</sup> Shaobo Wang,<sup>4,15,6</sup> Shibo Wang,<sup>17</sup> Siguang Wang,<sup>22</sup> Wei Wang,<sup>9,19</sup> Xu Wang,<sup>1</sup> Zhou Wang,<sup>1,5,6</sup> Yuehuan Wei,<sup>9</sup> Weihao Wu,<sup>4,6</sup> Yuan Wu,<sup>4</sup> Mengjiao Xiao,<sup>4</sup> Xiang Xiao,<sup>19</sup> Kaizhi Xiong,<sup>7,6</sup> Jianqin Xu,<sup>4</sup> Yifan Xu,<sup>17</sup> Shunyu Yao,<sup>15</sup> Binbin Yan,<sup>1</sup> Xiyu Yan,<sup>26</sup> Yong Yang,<sup>4,6</sup> Peihua Ye,<sup>4</sup> Chunxu Yu,<sup>23</sup> Ying Yuan,<sup>4</sup> Zhe Yuan,<sup>11</sup> Youhui Yun,<sup>4</sup> Xinning Zeng,<sup>4</sup> Minzhen Zhang,<sup>1</sup> Peng Zhang,<sup>7,6</sup> Shibo Zhang,<sup>1</sup> Siyuan Zhang,<sup>19</sup> Shu Zhang,<sup>19</sup> Tao Zhang,<sup>1,5,6</sup> Wei Zhang,<sup>1</sup> Yang Zhang,<sup>2,3,†</sup> Yingxin Zhang,<sup>2,3</sup> Yuanyuan Zhang,<sup>1</sup> Li Zhao,<sup>1,5,6</sup> Kangkang Zhao,<sup>1</sup> Jifang Zhou,<sup>7,6</sup> Jiaxu Zhou,<sup>15</sup> Jiayi Zhou,<sup>1</sup> Ning Zhou,<sup>1,5,6</sup> Xiaopeng Zhou,<sup>8</sup> Zhizhen Zhou,<sup>4</sup> and Chenhui Zhu<sup>18</sup>

(PandaX Collaboration)

<sup>1</sup>State Key Laboratory of Dark Matter Physics, Key Laboratory for Particle Astrophysics and Cosmology (MoE), Shanghai Key Laboratory for Particle Physics and Cosmology, Tsung-Dao Lee Institute & School of Physics and Astronomy, Shanghai Jiao Tong University, Shanghai 201210, China

<sup>2</sup>Research Center for Particle Science and Technology, Institute of Frontier and Interdisciplinary Science, Shandong University, Qingdao 266237, China

<sup>3</sup>Key Laboratory of Particle Physics and Particle Irradiation of Ministry of Education, Shandong University, Qingdao 266237, China

<sup>4</sup>State Key Laboratory of Dark Matter Physics, Key Laboratory for Particle Astrophysics and Cosmology (MoE), Shanghai Key Laboratory for Particle Physics and Cosmology, School of Physics and Astronomy, Shanghai Jiao Tong University, Shanghai 200240, China

<sup>5</sup>Shanghai Jiao Tong University Sichuan Research Institute, Chengdu 610213, China

<sup>6</sup>Jinping Deep Underground Frontier Science and Dark Matter Key Laboratory of Sichuan Province, Liangshan 615000, China

<sup>7</sup>Yalong River Hydropower Development Company, Ltd., 288 Shuanglin Road, Chengdu 610051, China

<sup>8</sup>School of Physics, Beihang University, Beijing 102206, China

<sup>9</sup>Sino-French Institute of Nuclear Engineering and Technology, Sun Yat-Sen University, Zhuhai 519082, China

<sup>10</sup>Department of Physics, Yantai University, Yantai 264005, China

<sup>11</sup>Key Laboratory of Nuclear Physics and Ion-beam Application (MOE), Institute of Modern Physics, Fudan University, Shanghai 200433, China

<sup>12</sup>Peng Huanwu Collaborative Center for Research and Education, Beihang University, Beijing 100191, China

<sup>13</sup>International Research Center for Nuclei and Particles in the Cosmos & Beijing Key Laboratory of Advanced Nuclear Materials and Physics, Beihang University, Beijing 100191, China

<sup>14</sup>Southern Center for Nuclear-Science Theory (SCNT), Institute of Modern Physics, Chinese Academy of Sciences, Huizhou 516000, China

<sup>15</sup>SJTU Paris Elite Institute of Technology, Shanghai Jiao Tong University, Shanghai 200240, China

<sup>16</sup>Department of Physics, University of Maryland, College Park, Maryland 20742, USA

<sup>17</sup>School of Mechanical Engineering, Shanghai Jiao Tong University, Shanghai 200240, China

<sup>18</sup>Department of Modern Physics, University of Science and Technology of China, Hefei 230026, China

<sup>19</sup>School of Physics, Sun Yat-Sen University, Guangzhou 510275, China

<sup>20</sup>*State Key Laboratory of Particle Detection and Electronics,  
University of Science and Technology of China, Hefei 230026, China*

<sup>21</sup>*New Cornerstone Science Laboratory, Tsung-Dao Lee Institute, Shanghai Jiao Tong University, Shanghai 201210, China*

<sup>22</sup>*School of Physics, Peking University, Beijing 100871, China*

<sup>23</sup>*School of Physics, Nankai University, Tianjin 300071, China*

<sup>24</sup>*School of Science, Sun Yat-Sen University, Shenzhen 518107, China*

<sup>25</sup>*College of Nuclear Technology and Automation Engineering, Chengdu University of Technology, Chengdu 610059, China*

<sup>26</sup>*School of Physics and Astronomy, Sun Yat-Sen University, Zhuhai 519082, China*

The landmark detection of neutrinos from SN 1987A marked the dawn of a new era in astrophysics, unequivocally establishing them as indispensable probes for investigating stellar evolution and supernova dynamics. Today, supernova burst neutrinos can be observed through coherent elastic neutrino-nucleus scattering in tonne-scale liquid xenon detectors designed for direct dark matter detection. Capitalizing on this capability, we have developed and deployed a real-time supernova monitoring system for the PandaX-4T experiment. This system incorporates a GPS module providing millisecond-level timing precision, achieves a low false-alarm rate, and maintains high sensitivity to galactic supernova events. This robust methodology is directly scalable and slated for implementation in the next-generation PandaX-20T experiment.

Core-collapse supernova explosions occur fewer than three times per century within the Milky Way [1]. The most recent neutrinos from a supernova (SN) explosion were detected from SN 1987A, with around 20 neutrino events in total observed by the global neutrino detectors [2–4]. The mechanism of supernova explosions has been explained by a series of theoretical models [5–7]. However, given the limited statistics, scientists have not yet fully understood the physical processes in supernova dynamics yet. To get prepared for the neutrino detection from next galactic supernova burst, a number of neutrino experiments have implemented specialized supernova monitoring systems [8–10].

Supernova bursts occur in the latter stages of evolution of massive stars with masses exceeding eight times that of the Sun. Roughly  $10^{53}$  erg of energy is released when a SN bursts, with neutrinos carrying away about 99% of the energy [11]. The entire explosion process takes about several seconds. Compared to electromagnetic radiations and gravitational waves, neutrinos generated in the stellar core can more easily escape the supernova interior and are emitted earlier, enabling them to reach ground-based observatories before the light and gravitational messengers [12]. Therefore, a global organization known as the Supernova Early Warning System (SNEWS) was established to provide the astronomical community with an early warning of SN explosions [13, 14].

The COHERENT experiment reported the first observation of coherent elastic neutrino nucleus scattering (CE $\nu$ NS) using neutrinos from a spallation neutron source in 2017 [15]. This observation provides an excellent opportunity for detecting astronomical neutrinos by CE $\nu$ NS [16, 17]. The CE $\nu$ NS cross-section is proportional to the square of the target nuclei’s neutron number,  $\sigma_{\nu} \simeq N^2 G_{\text{F}}^2 E_{\nu}^2 / 4\pi$ , where  $N$  is the neutron number of the target nucleus,  $G_{\text{F}}$  is the Fermi coupling constant, and  $E_{\nu}$  denotes the neutrino energy [18]. Because the xenon target nucleus contains around 80 neutrons, it is a suitable choice for a direct detection experiment of dark matter utilizing liquid xenon, such as XENONnT/LUXZEPLIN [9, 19], to detect SN neutrinos by CE $\nu$ NS. The neutral current process makes this interaction sensitive to all neutrino flavors, and the neutrino oscillation is not necessary to be taken into account. It can also complement the findings from other experiments that are particularly sensitive to only one or several specific flavors of neutrinos [20, 21]. On the other hand, detecting neutrinos via CE $\nu$ NS is seriously hampered by the low nuclear recoil energy of  $\sim$ keV level.

The PandaX-4T experiment is located in the China Jinping Underground Laboratory (CJPL), with 2,400 m of rock overhead. Comprehensive knowledge about the detector can be found in Ref. [22], and only a few essential details are described in the Letter. The primary detector is a cylindrical xenon time projection chamber (TPC), containing approximately 3.7 tonnes of liquid xenon (LXe). Physical events are reconstructed according to the coincidence detection of photons from prompt

\* Spokesperson: jianglai.liu@sjtu.edu.cn

† Corresponding author: yangzhangsdu@email.sdu.edu.cn

scintillation (S1) and delayed electroluminescence photons from ionized electrons (S2). The top PMT pattern and the time difference between S1 and S2 are used to reconstruct the 3D interaction vertex, which can further suppress the external background through fiducialization.

Precise measurement of signal arrival times in the detector is crucial for tracking the SN by time-delay triangulation, which requires combining data from several observatories. A millisecond-level GPS-based timing system was specially designed for PandaX-4T, as shown in Fig. 1, to facilitate collaborative early warnings of SN explosions with other neutrino experiments globally. The GPS ground sub-system comprises a GPS receiver and a camp control module. The GPS antenna receives satellite signals and transmits them to the GPS server, which generates a high-precision 10 MHz reference clock through its internal clocking mechanism to synchronize the local clock of the control module. The precise GPS time, encoded in the IRIG-B code and synchronized with the one pulse per second (PPS) signal, is transmitted to the control module in the underground laboratory (hereafter referred to as lab control module) through a multi-kilometer optical fiber network. A hardware clock counter of the lab control module synchronizes with the DAQ's master clock at the start of each new data acquisition run, and the mapping between the delivered GPS time and the hardware clock ticks is stored in a database. The time delay introduced by the fiber optic length is determined by measuring the time difference between the emission and reception of synchronized time signals (e.g., 1 PPS pulses) between the camp control module and the lab control module. This delay is utilized to correct timestamps during data acquisition. The precision of this system is maintained at the millisecond level, which is determined primarily by the GPS server.

The PandaX-4T has been in operation since November 2020 and is scheduled to continue the data taking until the end of 2025. To improve the detection time accuracy of SN explosions, a dedicated GPS-based timing system as described above was established in July 2025.

Using the transient increase in detector signals induced by neutrinos from supernova explosions, PandaX-4T has developed an online software-based monitoring system to identify SN events, as illustrated in Fig. 2. When the DAQ system writes a new raw data file, the acquired data is subsequently stored utilizing the Bamboo Shoot3 library [23]. This library offers capabilities for

custom formatting and compression of commonly used data structures, enabling efficient data management and storage [24]. Each raw file contains roughly one minute of data and is approximately 2 GB in size. The data transformation process takes about ten seconds and compresses the data size to approximately 1 GB. Then, the data is transmitted to the remote data center in Chengdu for offline processing and reconstruction, which takes about 5 minutes. After event reconstruction, information of each recorded event, including interaction vertex coordinates, S1 and S2-related variables, etc., is derived. Next, the SN neutrino cut, including the dead time cut which refers to a period of time removed after large signals, the fiducial volume (FV) cut, the accidental coincidence (AC) cut, and quality cuts for S1 and S2, etc., is applied to further reduce the background and the surviving events serve as SN neutrino candidates to investigate false alert rates. The monitoring results indicate that the background event rate is stable. Finally, the SN trigger algorithm is utilized to identify potential SN explosion events. An alert will be generated when the number of neutrino candidates exceeds the threshold  $N_{thr}$  ( $N_{thr} = 2$ ) within a 10-second time window. Further details on this method can be found in Ref. [25]. The SN warning information, including the start time of the alert and the total number of neutrino candidates, etc., will be sent to the PandaX-4T SN group via email. It takes approximately 5 seconds to complete the process from selecting SN neutrino candidates to sending out an alert. The operational status of the SN monitoring system can be displayed on a webpage, allowing relevant personnel to inspect key parameters (e.g., event rate). Accounting for the aforementioned latency factors, the entire monitoring process takes approximately 6 minutes. The system sustains stable operation during routine data-taking periods, except in exceptional circumstances, such as power outages or server maintenance. In addition, during the calibration process, the SN monitoring program automatically excludes calibration-related data based on its data type.

The background in the detector is almost negligible over a time window of a few seconds. Practically, the background event rate in PandaX-4T is estimated to be approximately  $2.9 \times 10^{-4} \text{ s}^{-1}$  after the supernova neutrino cuts, resulting in a false alert rate of about twice per month. The majority of these backgrounds are electron recoil (ER) events, which, similar to previous analyses [26], comprise the material radioactivity, environ-

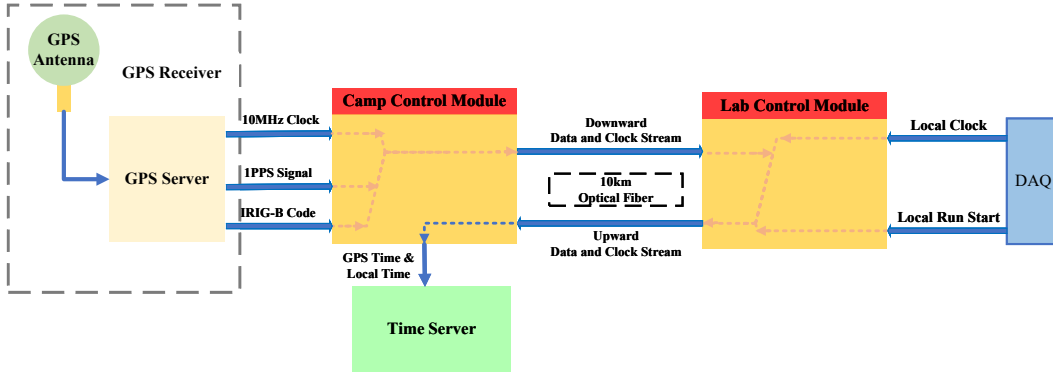


FIG. 1. Schematic diagram of the PandaX-4T’s GPS-based timing system.

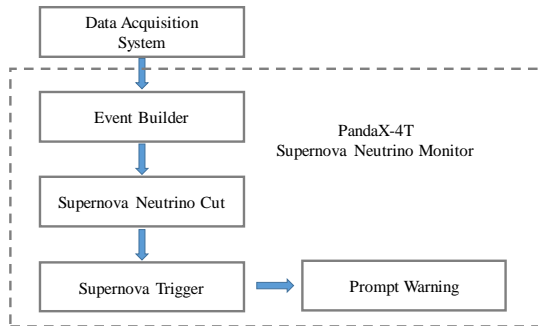


FIG. 2. Schematic diagram of SN online monitoring system in PandaX-4T.

mental radioactivity, AC events, and xenon contaminants (e.g.,  $^{222}\text{Rn}$ ). In about 83 days of physics data, six alerts are expected and eight are observed, which are in good agreement. Further verification of the consistency between the expectation and the observation is carried out with neutron calibration data from deuteron-deuteron (DD) and AmBe. The results show that 886 (288) alerts are observed for approximately 2.8 (3.7) days of the DD (AmBe) data, compared to 870.6 (265) expected alerts, corresponding to the background event rate of roughly  $2.2 \times 10^{-2}$  ( $9.7 \times 10^{-3}$ )  $\text{s}^{-1}$ . The algorithm of the expectation can be found in Ref. [25]. Regarding DD and AmBe data, scenarios where calibration event candidates are present in two separate files are taken into account, while for physics data, this can be ignored due to the lower background event rate. In the future, the false alert rate can be further reduced by lowering the background level, including using low-radioactivity materials in the detector and enhancing the removal efficiency of radioactive elements through a distillation tower.

Detection efficiency can be obtained via the pseudo data based on the simulation and “assembled” real detector waveforms and verified through calibration data, which is the same as the approach adopted in Refs. [26–28]. The signal model for PandaX-4T is built with the Noble Element Simulation Technique (NEST) v2.3.6 parameterization [29], and the relevant parameters are tuned by fitting calibration data [30]. The NEST model can simulate the light yield ( $L_y$ , number of photons per keV) and charge yield ( $Q_y$ , number of electrons per keV) of nuclear recoil events in LXe. Waveform simulation (WS) is developed using a data-driven simulation program in PandaX-4T, which generates complete waveforms of signals and background using  $L_y$  and  $Q_y$  as inputs [31]. The simulated events are reconstructed using the same methods as the experimental data.

The overall efficiency comprises the efficiencies of signal reconstruction, data quality selection, and region-of-interest (ROI). The signal reconstruction efficiency is similar to that discussed in the previous analysis [25]. Data quality selection mentioned earlier is inherited from the previous WIMP analysis [26], with slight adjustments made to adapt to the current data set. The ranges of S1 and S2 charges in the ROI are changed to [2.1, 100] PE and [80, 4000] PE to balance the false alert rate due to background contributions and detection efficiency of the nuclear recoil events induced by SN neutrinos. The efficiency of the dead time cut is estimated to be 89%, representing the surviving probability of the live time. The overall detection efficiency of SN neutrino events using the Garching model of  $M_p = 27 M_\odot$  described in the following paragraph is 13%.

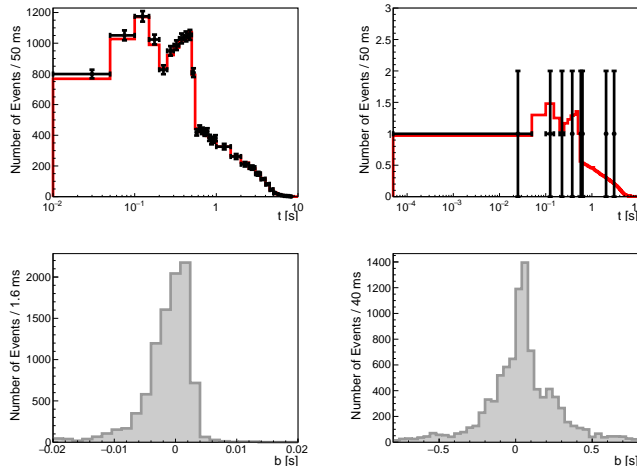


FIG. 3. Typical timing distributions of the detected supernova neutrino events from the distance of 168 pc (top left) and 10 kpc (top right). Data points are produced by simulations and the red lines are the fit results. The fitted onset times relative to the truth time in 10,000 simulated measurements are shown in the bottom panels. The resulting onset time measurement exhibits a variation of  $[-2.7, 2.4]$  ms and  $[-0.38, 0.11]$  s relative to zero for 168 pc and 10 kpc, respectively, within a 68% confidence level (C.L.).

The electroweak neutral current process allows neutrinos to coherently interact with all nucleons in the nucleus when their energy is very low ( $E_\nu \lesssim 100$  MeV). The differential cross-section calculation is detailed in Ref. [25]. To investigate the nuclear recoil signals induced by supernova neutrinos in PandaX-4T, supernova models are used to obtain the neutrino flux as input. In this work, we adopt two Garching models with  $M_p = 11.2 M_\odot$  and  $M_p = 27 M_\odot$ , employing the LS220 nuclear equation of state (EoS) [32, 33]. More information is available in the earlier publication [25]. Subsequently, the differential event rate of CE $\nu$ NS can be expressed as

$$\frac{dN^2}{dE_{\text{nr}} dt_{\text{pb}}} (E_{\text{nr}}) = \frac{m_{\text{det}} N_A}{M_A (4\pi d^2)} \int_{E_\nu^{\text{min}}}^{\infty} \frac{d\sigma}{dE_{\text{nr}}} (E_\nu, E_{\text{nr}}) \times \Phi(E_\nu, t_{\text{pb}}) \epsilon(E_{\text{nr}}) dE_\nu, \quad (1)$$

where  $t_{\text{pb}}$  represents the time after the SN core bounce,  $m_{\text{det}} = 2.6$  tonnes is the effective target mass in this analysis,  $N_A$  is Avogadro's number, and the molar mass of xenon is  $M_A = 131.2$  g/mol, and  $d$  is the distance from the SN to Earth.  $E_\nu^{\text{min}} = \sqrt{m_A E_{\text{nr}}/2}$  represents the minimum neutrino incident energy required to induce a nuclear recoil energy of  $E_{\text{nr}}$  in CE $\nu$ NS. In practice, we integrate over  $E_\nu \in (E_\nu^{\text{min}}, 300 \text{ MeV})$ .  $d\sigma/dE_{\text{nr}}$  and  $\Phi(E_\nu, dt_{\text{pb}})$  are the differential cross-section of the CE $\nu$ NS process and the total neutrino fluxes of all flavors at the energy of  $E_\nu$  and time of  $t_{\text{pb}}$ , respectively.

$\epsilon(E_{\text{nr}})$  represents the detection efficiency.

The core bounce onset time can be determined when sufficient event statistics are available. A typical fitting result of the timings after the core bounce of the supernova neutrino events from the distance of 168 pc is displayed in the top left panel of Fig. 3. The points represent the simulated SN neutrino events, and the histogram represents the fitting result using the equation  $a \cdot f(t - b)$ , where  $f$  denotes the differential time profile of the SN events, while  $a$  and  $b$  signify the amplitude and time shift of the time profile, respectively, which are free parameters. The bottom left panel of Fig. 3 illustrates the distribution of parameter  $b$ , indicating a discrepancy in the core bounce time of SN explosions between the simulated measurements and the theoretical predictions. The case of 10 kpc is shown in the right panels of Fig. 3. The 68% C.L. intervals for the variation of the offset times relative to the zero are  $[-2.7, 2.4]$  ms at 168 pc and  $[-0.38, 0.11]$  s at 10 kpc due to smaller statistics.

The expected number of SN neutrino events in the detector can be calculated by integrating Eq. 1. Here, we integrate the variable  $t_{\text{pb}}$  for the model with  $M_p = 27 M_\odot$  ( and  $M_p = 11.2 M_\odot$  ) over the time interval from the onset time of core bounce to 8.35 (7.6) seconds.  $E_{\text{nr}}$  is integrated up to 30 keV. The results indicate that the number of the expected SN neutrinos from 10 kpc (168 pc) in PandaX-4T is approximately 8.1 ( $2.9 \times 10^4$ ) and 3.7 ( $1.3 \times 10^4$ ) for the model of  $M_p = 27 M_\odot$  and

$M_p = 11.2 M_\odot$ , respectively. Only the results for the case of  $M_p = 27 M_\odot$  is shown in Fig. 3 for simplicity. The distances of 10 kpc and 168 pc correspond to the positions of the nearby Galactic center and Betelgeuse [34] as observed from Earth, respectively.

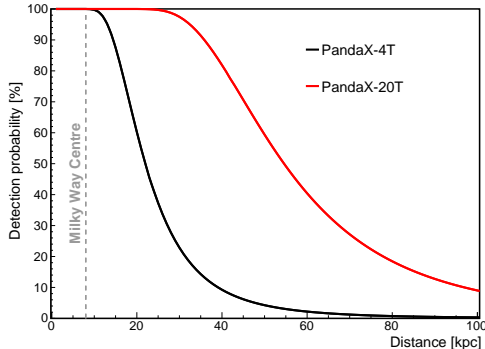


FIG. 4. Detection probability of the SN explosions as a function of distance using the Garching model with  $M_p = 27 M_\odot$  for PandaX-4T (black) and PandaX-20T (red). The corresponding false alert rate is twice a month in PandaX-4T.

The detection probability of SN explosions is estimated using the Garching model with  $M_p = 27 M_\odot$ , employing the LS220 EoS. Figure 4 illustrates the detection probability as a function of SN distance to the PandaX-4T and PandaX-20T. PandaX-4T achieves nearly-100% detection efficiency at 10 kpc, while the PandaX-20T with the effective target mass enlarged by a factor of about

6 to  $\sim 16$  tonnes, maintains  $\sim 100\%$  efficiency up to 30 kpc.

SNEWS significantly improves the confidence of SN explosion warnings through coincident onset times of alerts from several collaborative experiments. The SNEWS system provides different message tiers for participating experiments, as listed in the first column of Table I. The second and third columns present the essential information for each tier and the corresponding values of a typical SN candidate alert in the PandaX-4T, respectively. The coincidence tier is a prerequisite for experiments to be incorporated in SNEWS. More details about SNEWS alert software are provided in Ref. [35]. The detector status parameter is set to ON/OFF according to its operational condition. The neutrino time is represented in UTC format, derived from GPS time in Pandax-4T. The time series is an ordered sequence of nanosecond-precision integers, representing the time offsets relative to the initial neutrino time. According to the background-only assumption, if two events are observed in the first 5-second time window, the p-value calculated via the Poisson distribution with expected rate  $\mu = \lambda t$  (where  $\lambda = 2.9 \times 10^{-4} \text{ s}^{-1}$  and  $t = 5 \text{ s}$ ) is  $6.11 \times 10^{-6}$ . In contrast, the p-value for observing greater than or equal to zero events is 1 in the second 5-second time window. Retraction is initiated via a dedicated command provided by the SNEWS network, based on real-time experimental considerations. The information shown in the third column of Table I satisfies the requirements of the SNEWS message tiers.

TABLE I. List of different message tiers within the SNEWS network. The detector name is required in each tier and is not listed in the column. The neutrino time is represented in UTC format. The p-value is calculated via the Poisson distribution for every 5-second time window. The units for the time bins and the neutrino time series (measured relative to the first event) are seconds and nanoseconds, respectively.

Tier	Required information	Value
Coincidence	initial neutrino time	2025-10-06T14:13:20.333181
Significance	p-values for time bins, width of time bins	[6.11e-06, 1.00], 5.00
Timing	initial neutrino time, neutrino time series	2025-10-06T14:13:20.333181, [0, 1213145668]
Heartbeats	detector status	ON/OFF
Retraction	retract latest	—

In summary, we have established an online supernova monitoring system with GPS time implemented at PandaX-4T. The monitoring system can provide the astronomical community with early warning of SN explosions and can achieve about 100% detection efficiency of SN explosions at 10 kpc in PandaX-4T, corresponding to a false alert rate of twice per month. Distinguishing

between different SN models would be possible using the distinct time profile and energy spectrum features if an SN burst were to occur at a close distance to Earth (e.g., Betelgeuse). In the near future, the PandaX-20T experiment is expected to significantly enhance the sensitivity to astronomical neutrinos, particularly those from core-collapse supernova in our galaxy and the Sun, thereby

enabling more precise tests of astrophysical models.

**Acknowledgements.** This project is supported in part by grants from National Key R&D Program of China (Nos. 2023YFA1606200, 2023YFA1606203), National Science Foundation of China (Nos. 12090060, 12090061, U23B2070), and by Office of Science and Technology, Shanghai Municipal Government (grant Nos. 21TQ1400218, 22JC1410100, 23JC1410200, ZJ2023-ZD-003). We thank for the support by the Discipline Con-

struction Fund of Shandong University, and the Fundamental Research Funds for the Central Universities. We also thank the sponsorship from the Chinese Academy of Sciences Center for Excellence in Particle Physics (CCEPP), Thomas and Linda Lau Family Foundation, New Cornerstone Science Foundation, Tencent Foundation in China, and Yangyang Development Fund. Finally, we thank the CJPL administration and the Yalong River Hydropower Development Company Ltd. for indispensable logistical support and other help.

- 
- [1] S.Horiuchi, J.F.Beacom, and E.Dwek 2009 Phys.Rev.D 79, 083013
  - [2] R.M.Bionta, G.Blewitt, C.B.Bratton et al. 1987 Phys.Rev.Lett 58, 1494
  - [3] K.Hirata, T.Kajita, M.Koshihara et al. 1987 Phys.Rev.Lett 58, 1490
  - [4] E.N.Alexeyev, L.N.Alexeyeva, I.V.Krivoshchina et al. 1988 Phys.Lett.B 205, 209
  - [5] S.E.Woosley, A.Heger and T.A.Weaver, 2002 Rev.Mod.Phys 74, 1015
  - [6] H.-T.Janka, K.Langanke et al. 2007 Phys.Rept. 442, 38
  - [7] Alexander Summa, Florian Hanke et al. 2016 Astrophys.J. 825, 6
  - [8] Y.Kashiwagi et al 2024 ApJ 970 93
  - [9] Kara, Melih 2025 Ph.D Dissertatio (Karlsruhe Institute of Technology)
  - [10] Angel Abusleme et al 2024 JCAP 2024 057
  - [11] D.Kresse, T.Ertl, and H.T.Janka 2021 ApJ 909 169
  - [12] K.Abe et al. 2016 Astroparticle Physics, 81 39
  - [13] P.Antonioli et al. 2004 New Journal of Physics 6, 114
  - [14] S Al Kharusi et al. 2021 New Journal of Physics 23, 031201
  - [15] Dmitry Akimov et al. 2017 Science 357, eaao0990
  - [16] Aprile, E. et al 2024 Phys.Rev.Lett 133, 191002
  - [17] Zihao Bo et al 2024 Phys.Rev.Lett 133, 191001
  - [18] A.M.Suliga, J.F.Beacom, and I. Tamborra 2022 Phys.Rev.D 105, 043008
  - [19] D.Khaitan 2018 JINST 13 C02024
  - [20] K.Bays et al. 2012 Phys.Rev.D 85, 052007
  - [21] J.F.Beacom and L.E.Strigari 2006 Phys.Rev.C 73035807
  - [22] H.G.Zhang et al. 2019 Science China(Physics, Mechanics & Astronomy) 62, 031011
  - [23] Lei, Siao and Chen, Xun <https://github.com/pandax-experiments/bamboo-shoot3>
  - [24] Yubo Zhou et al 2024 JINST 19 P05029
  - [25] Binyu Pang, et al. 2024 Chin.Phys.C 48, 073002
  - [26] Zihao Bo, et al. 2025 Phys.Rev.Lett 134, 011805
  - [27] Ma, Wenbo et al. 2023 Phys.Rev.Lett. 130, 021802
  - [28] Zihao Bo et al. 2024 Phys.Rev.Lett. 133, 191001
  - [29] M.Szydagis et al. Noble Element Simulation Technique v2.0. 2018
  - [30] Luo, Yunyang et al. 2024 Phys.Rev.D 110, 023029
  - [31] J. Li et al. 2024 Chin.Phys.C 48, 073001.
  - [32] A.Mirizzi, I.Tamborra, H.Th.Janka et al. 2016 Nuovo Cimento Rivista Serie 39
  - [33] L. Hüdepohl 2014 Ph.D. Dissertation ( Max Planck Institute )
  - [34] M.Joyce, S.C.Leung, L.Molná et al. 2020 The Astrophysical Journal 902(1), 63 (2020)
  - [35] M. Kara et al 2024 JINST 19 P10017